DOE Award DE-FE0031548

High Temperature Electrochemical Sensors for In-situ Corrosion Monitoring In Coal-Based Power Generation Boilers

Xingbo Liu, Debangsu Bhattacharyya, Shanshan Hu, Tianliang Zhao, Liang Ma
West Virginia University

Brandon Rumberg
Aspinity

Jared Custer, Chad Hufnagel
Longview Power

OUTLINE

- Technical Background
- Project Objectives
- Field Test Results
- Reference Electrode Development
- Corrosion Database Development
- Techno-Economical Analysis Progress
- Summary and Future Work
- Acknowledgement

Hot Corrosion Mechanism

Hot corrosion: the degradation of an alloy at elevated temperature induced by a thin molten salt layer under an oxidizing atmosphere.

O_2-SO_2-SO_3

Sulfate salt	Tm (°C)
Na_2SO_4	884
K_2SO_4	1069
Na_2SO_4-$CoSO_4$	575
K_2SO_4-$CoSO_4$	535
$K_3Fe(SO_4)_3$	624
$Na_3Fe(SO_4)_3$	618
$Na_2S_2O_7$	400.9
$K_2S_2O_7$	325

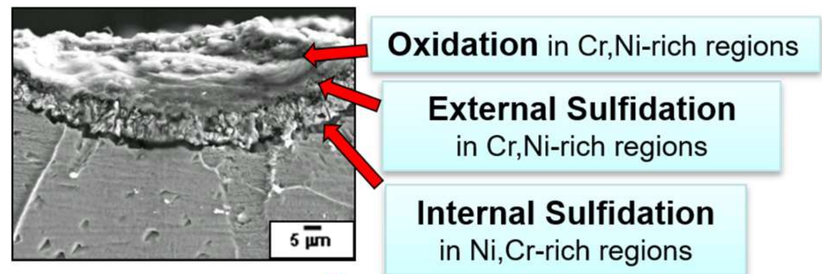

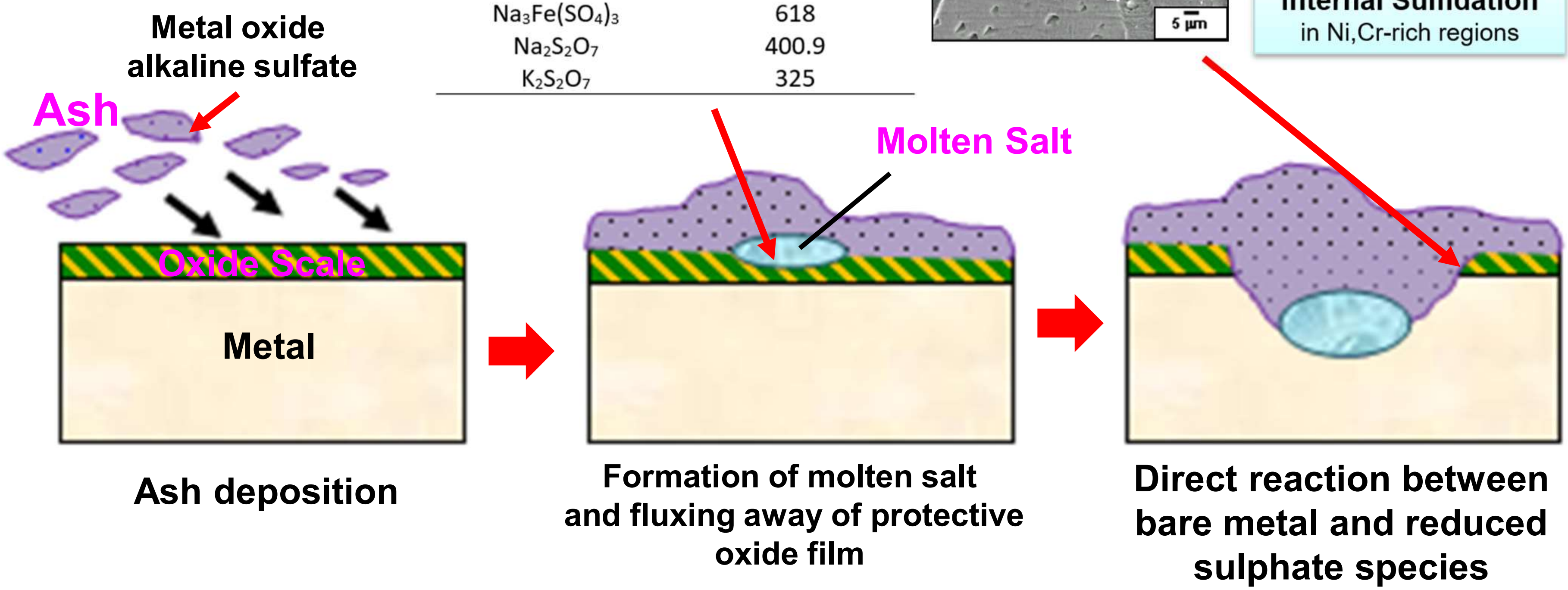

Schematic of hot corrosion mechanism induced by coal ash

Aung, Naing Naing, and **Xingbo Liu***. Corrosion science 76 (2013): 390-402.

Reproducibility of Potential and Current Signals During Oxidation and Sulfidation

Both potential and current noise are effective and efficient signals to reveal the stages of corrosion process (oxidation and sulfidation) in the simulated coal-fired power plant environment.

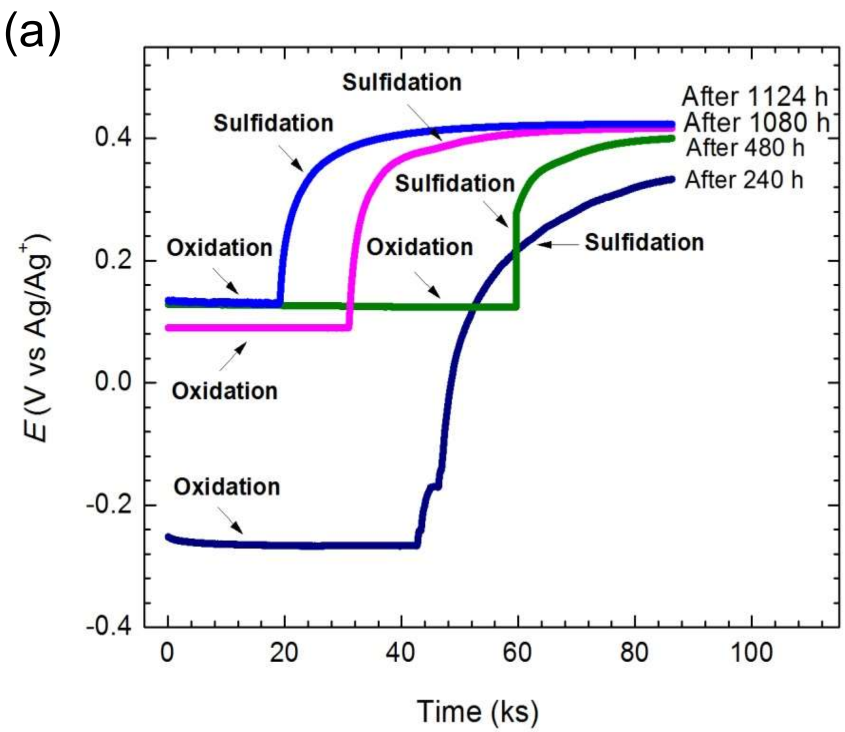

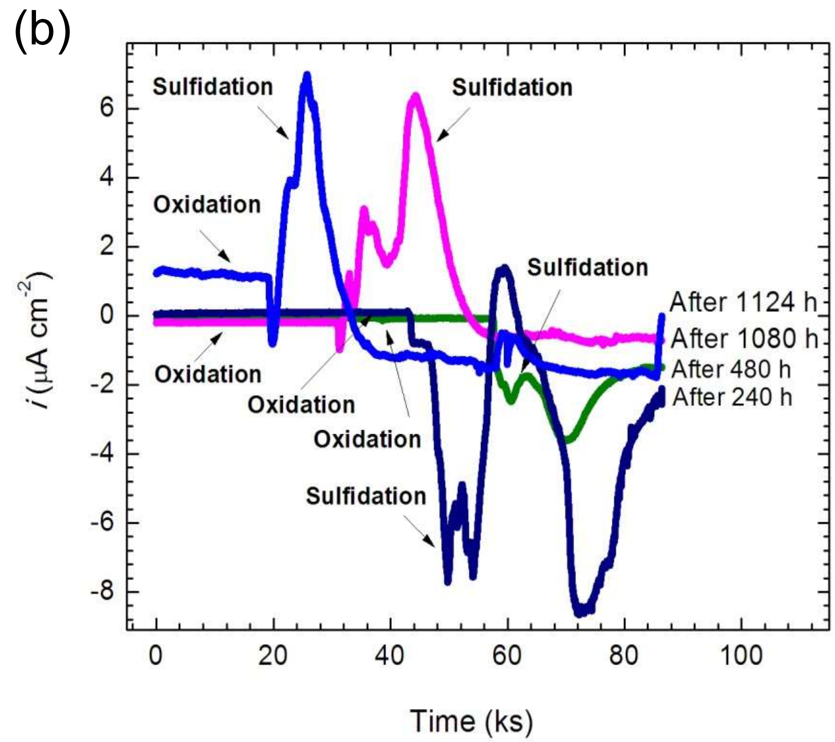

(a) potential and (b) current noise signals obtained for Inconel 740 alloy beneath a thin layer of coal ash at 850 ^oC

Aung, Naing Naing, Edward Crowe, and **Xingbo Liu***. ISA transactions 55 (2015): 188-194.

FIVE Typical Noise Signals Measured in the Coal Ash Hot Corrosion Process

Electrochemical Potential Noise Signals

- The noise signature of a gradual potential continuously changing in the negative region ***(Noise Signature I)*** corresponded with the Oxidation Stage
- The noise signature of quick potential continuously approaching more positive values ***(Noise Signature II)*** correlated to the External Sulfidation Stage.
- The noise signature of positive potential fluctuating randomly in a narrow range ***(Noise Signature III)*** corresponded with the Internal Sulfidation Stage

Electrochemical Current Noise Signals

- The noise pattern of the noise signature of current fluctuating with no sudden spike correlated to the Low Extent of Oxidation/Sulfidation ***(Noise Signature IV)***.
- The noise pattern of sudden change in current values followed by slow or no recovery corresponded with the Accelerated Oxidation/Sulfidation ***(Noise Signature V)***. These signatures can be seen clearly at 750 °C, in the flue gas without SO_2 as well as deep coal ash.

Aung, Naing Naing, and **Xingbo Liu***. Corrosion science 82 (2014): 227-238.

Sensor Testing @ Prototype Boiler

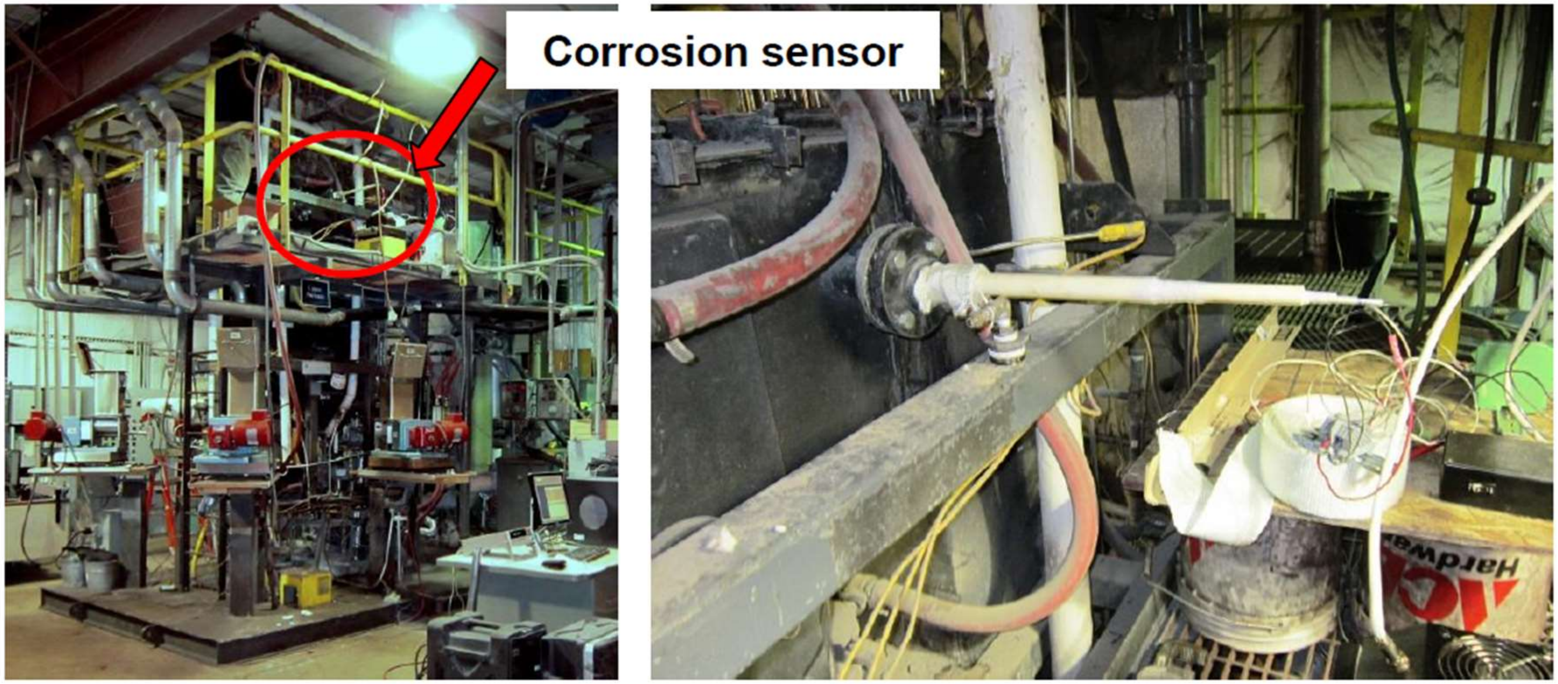

Corrosion and Wireless Sensor Location at WRI's Combustion Test Facility

Photographs of WVU high temperature corrosion sensor: (a) new sensor; (b) sensor 45 days post-exposure in boiler at WRI's Combustion Testing Facility

Project Objectives

- To validate the effectiveness of our Recipient's lab-scale electrochemical sensor for high temperature (HT) corrosion in coal-based power generation boilers;
- To optimize the Recipient's HT sensor (currently at technology readiness level TRL-5) to reach TRL-6;
- To develop a pathway toward commercialization of such technology.

Sensor Testing Locations

Superheater/reheater tubes working conditions: high temperature and pressure (550-750^{o}C, 30MPa), high salt concentration (Na_2SO_4,K_2SO_4), corrosive flu gas (O_2, SO_2 and SO_3)

Component: Nickel-based alloys (e.g., 282, 740) or fire-resistant stainless steel (e.g., 347H).

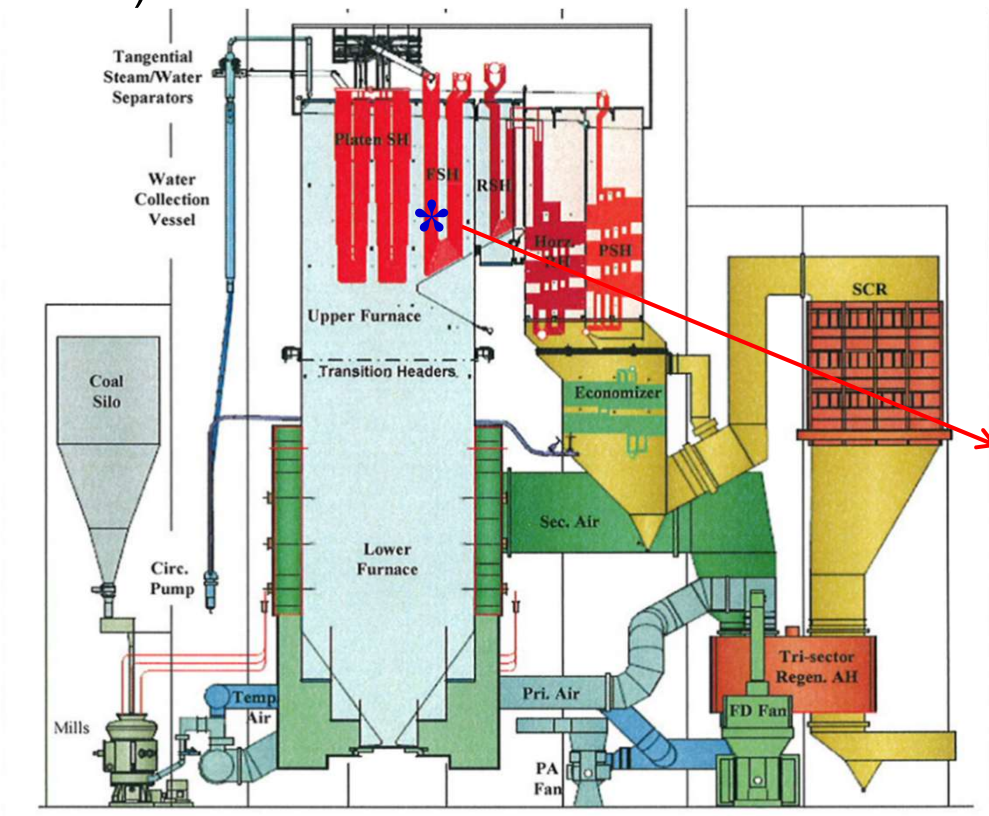

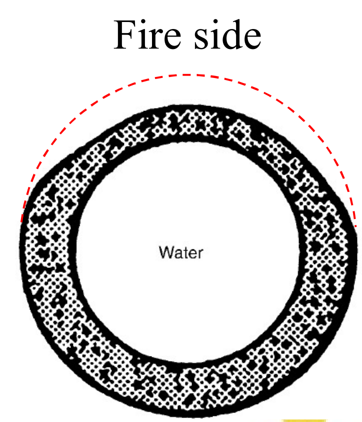

Sensor Packaging-Data Acquisition System

- ✓ This data acquisition system has a reliable accuracy.
- ✓ The latest version also enables remote data collection (developed in Feb 2020).

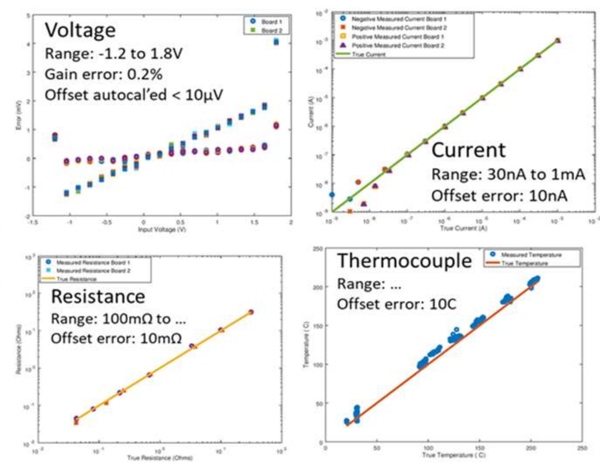

[Left] PIECES hardware. (a) Top view of the fully-assembled device. (b) Bottom view of the Front Panel. (c) Top view of the Measurement Board. [Right] Verification of each measurement type.

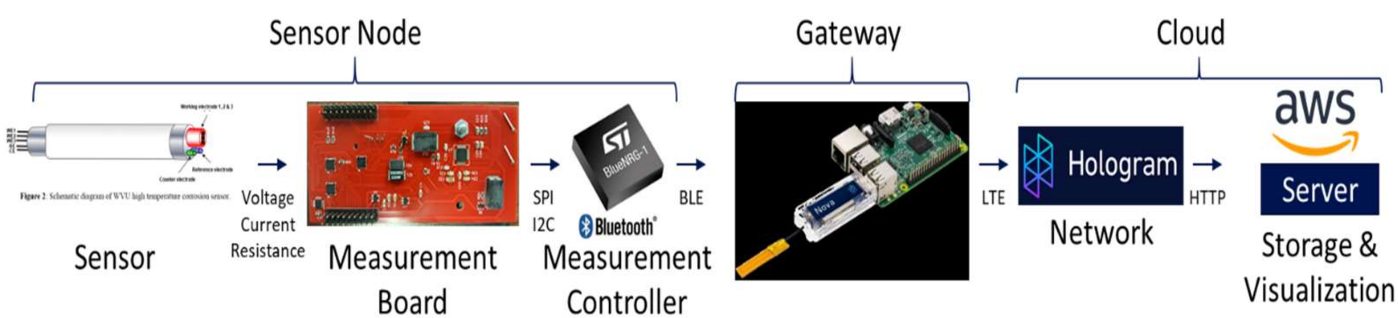

Envisioned data pipeline for the corrosion sensor.

Sensor Placing and Installation-ECN Sensor

✓ An updated electrochemical sensor was successfully installed on Aug 30th, 2019

Electrochemical sensor

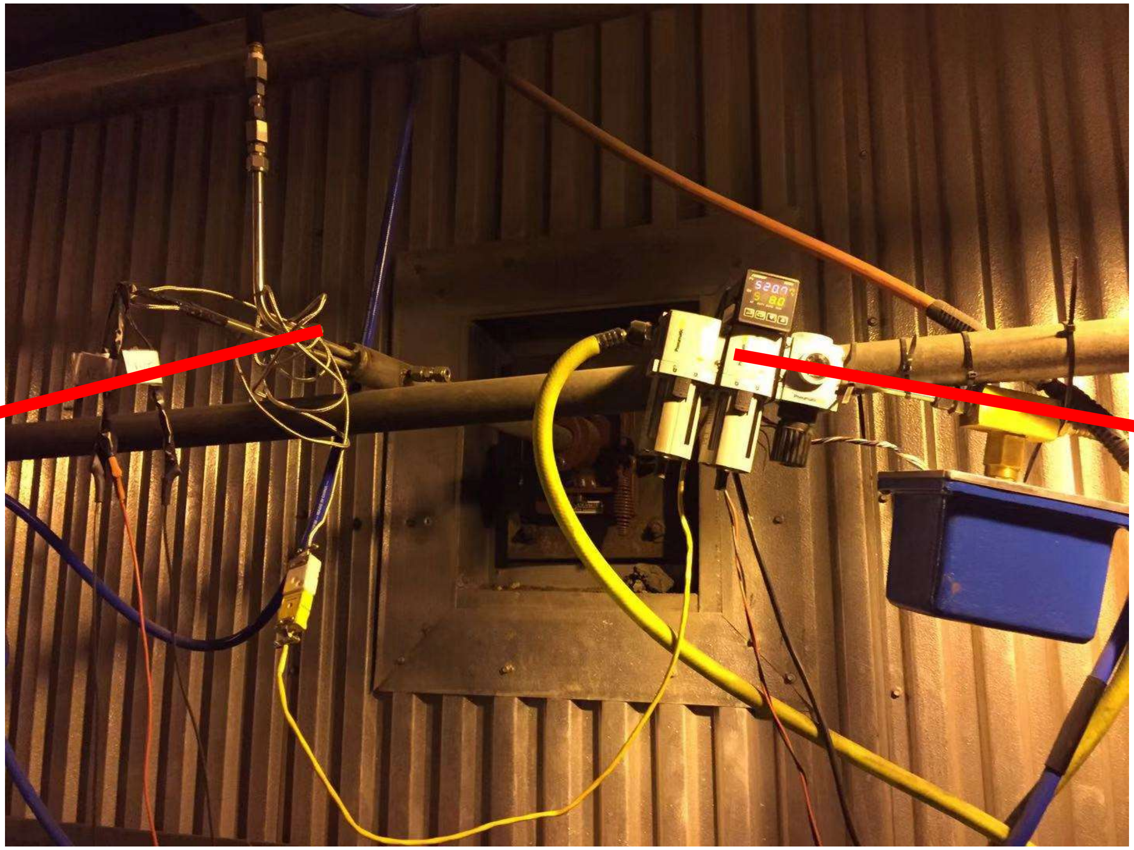

Temperature Controller (550 ^{o}C)

ECN sensor system installed through the observation port near superheater (11th floor of the boiler).

Field Measurement Results-PDP curves

- ✓ PDP curve was successfully obtained after 1d, demonstrating the formation of molten salt layer on 347H SS.
- ✓ Stern-Geary coefficient was calculated from PDP curve as 69.78.

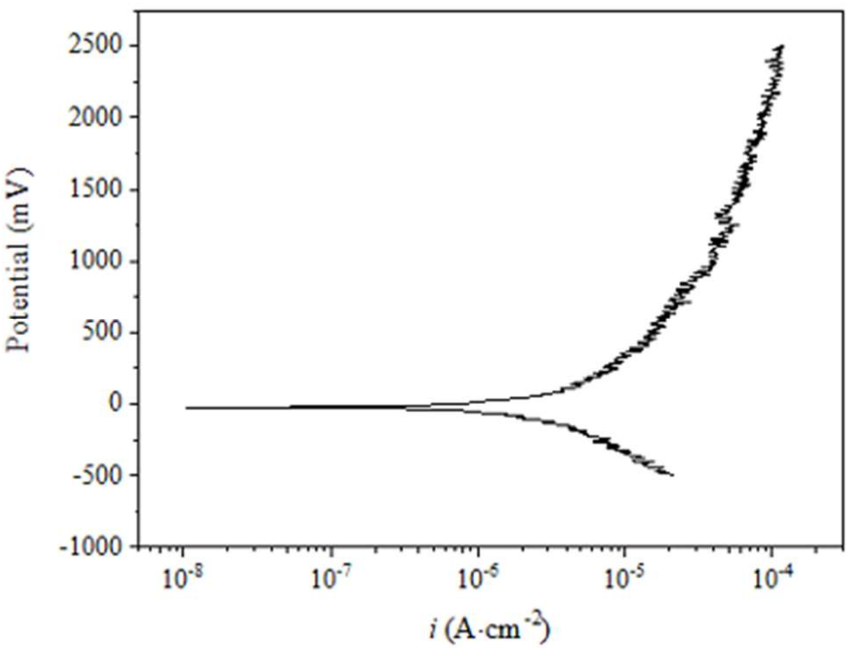

The potentiodynamic polarization (PDP) curve of 347H SS measured at superheater place (550ºC)

Parameters obtained from the PDP

Materials and location	Anodic Tafel slope, α (mV/decade)	Cathodic Tafel slope, β (mV/decade)	Stern-Geary coefficient, B (mV)
347 SS, Superheater	810.08±159.98	200.49±17.72	69.78

Anodic reaction: $Fe - 3e^{-} \rightarrow Fe^{3+}$

n=3, ρ=7.8 g/cm^3, M=56 g/mol

Predictive Model Development-Calculations of Corrosion Rate

✓ Corrosion depth can be calculated by EN data through eq. (6).

Measure PDP Reference Curve using an Electrochemical Workstation

↓

Calculate the Tafel Slope from the PDP Reference Curve using Eq. 1

↓

Calculate the Corrosion Current using Eq. 2

↓

Calculate the Corrosion Rate using Eq. 3

Measure Potential Noise and Current Noise by Voltmeter and Ammeter

↓

Calculate the Noise Resistance from the Potential Noise and Current Noise using Eq. 4

↓

Replace Polarization resistance (R_p) by Noise Resistance (R_n)

↓

Calculate the Corrosion Rate using Eq. 5

Introduce constants $M = 56, n = 3, \rho$=7.874, B=69.78

↓

Calculate Corrosion Rate using Eq. 6

$$B = \frac{\alpha\beta}{\alpha+\beta} \quad (1)$$

$$J_{corr} = \frac{B}{R_p} \quad (2)$$

$$V_{corr} = \frac{3.27 \times B \times M}{n \times \rho \times R_p} \quad (3)$$

$$R_n = \frac{\sigma_v}{\sigma_i} \quad (4)$$

$$V_{corr} = \frac{3.27 \times B \times M}{n \times \rho \times R_n} \quad (5)$$

$$V_{corr} = \frac{540.9}{R_n} \quad (6)$$

Processes to calculate the corrosion depth by electrochemical noise data

Field Measurement Results-ECN Data

- ✓ The latest electrochemical sensor works well in the last seven month.
- ✓ EN data was successfully collected unless the boiler is down

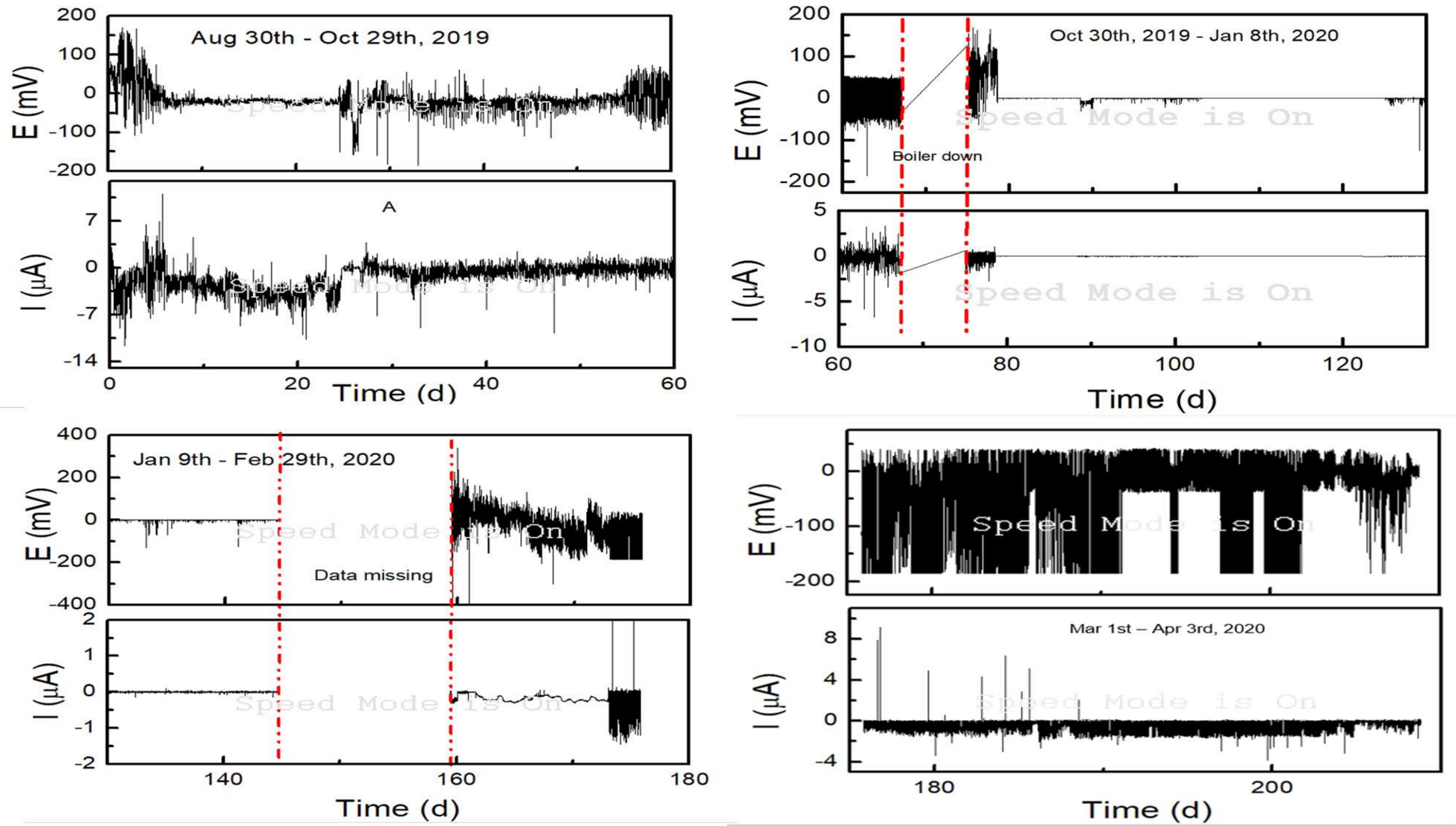

Electrochemical noises measured at the superheater (548ºC) since Aug 30th, 2019.

Field Measurement Results – Corrosion Rates

- ✓ The corrosion depth calculated by EN data is about mm in last six month.

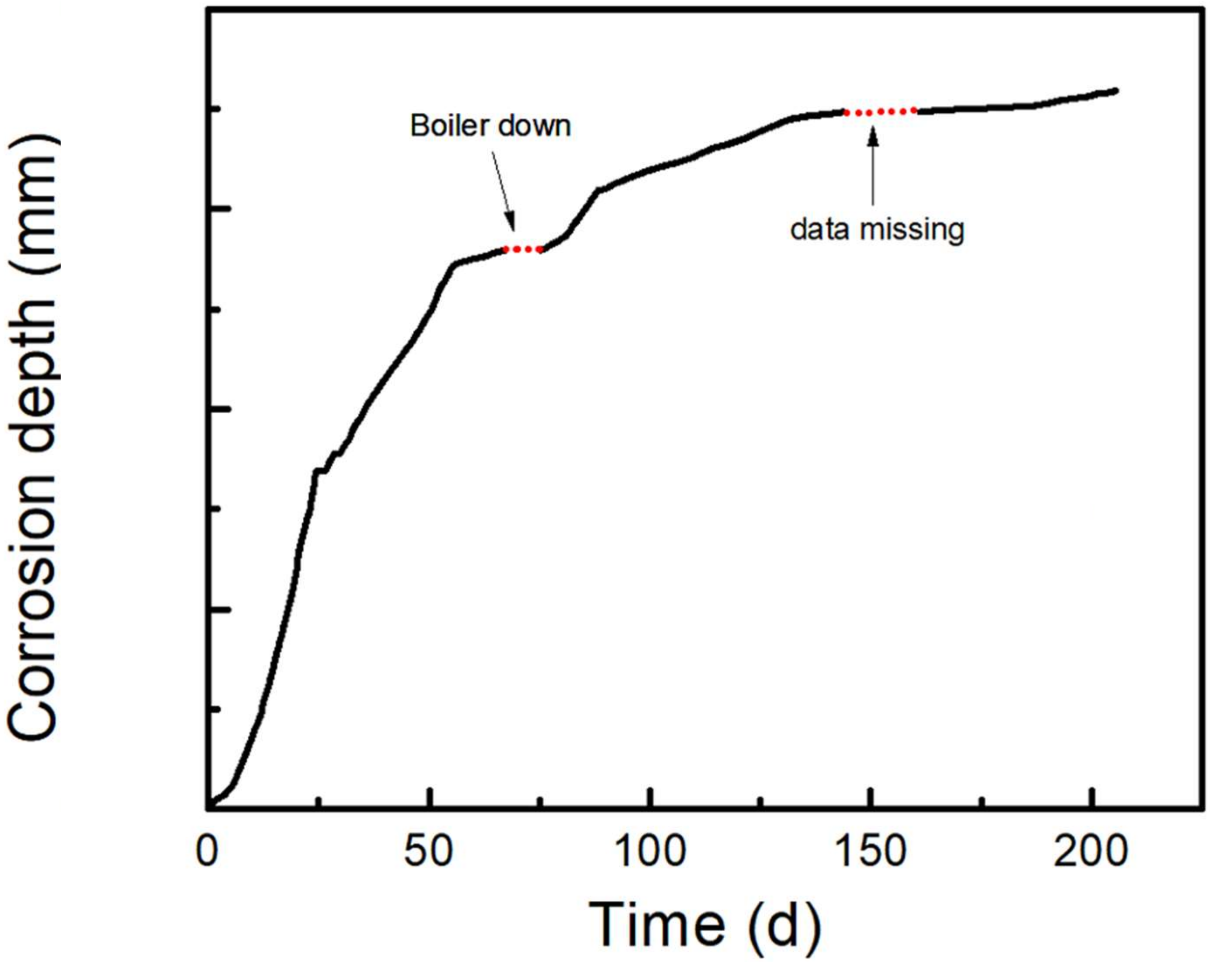

Time dependence of the accumulated corrosion depth calculated from the electrochemical noises measured at the superheater place.

Corrosion Database Development-Experiment Conditions

- ✓ Two kinds of coal ashes have different crystal structures.
- ✓ The main elements in both sets of coal ash are O, Al, Si, Fe, Ca, Na, K

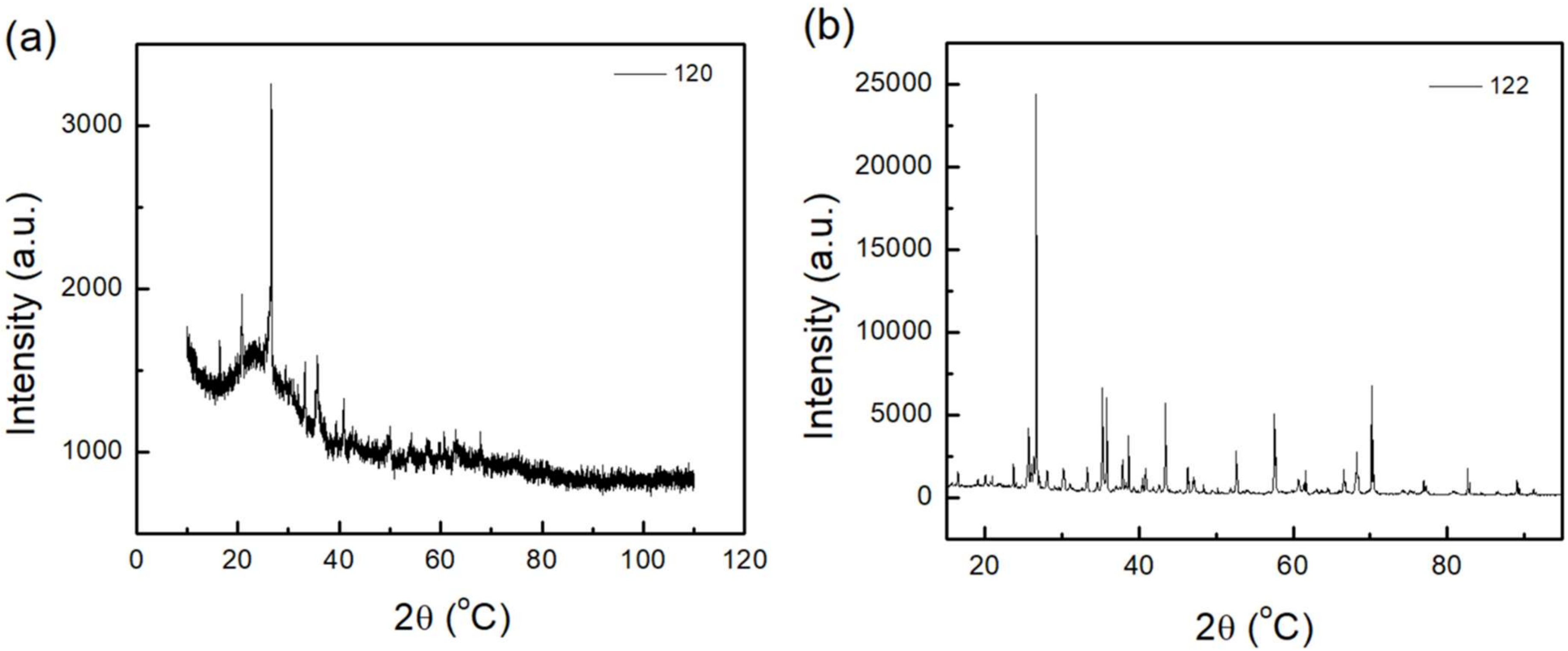

XRD pattern of two kinds of coal ashes obtained from Longview Power Plant

Corrosion Database Development-Experiment Conditions

- ✓ Some alkaline sulfate (Na_2O, K_2O and SO_3) was confirmed in both kinds of coal ashes
- ✓ Some metal oxides are found in both coal ashes
- ✓ Analysis result is similar to others reported in the literature

Various oxides in two kinds of coal ashes from Longview

	Al_2O_3	CaO	Fe_2O_3	MgO	MnO	P_2O_5	K_2O	SiO_2	Na_2O	SO_3	TiO_2
120	20.88	5.18	11.82	1.15	0.05	0.23	2.26	49.17	0.64	0.92	0.99
122	61.46	2.33	0.62	0.08	0.01	0.20	0.10	27.81	0.21	0.08	1.38

Representative chemical compositions of the coal ash in Literature

Al_2O_3	Fe_2O_3	SiO_2	Na_2SO_4	K_2SO_4	NaCl	$CaSO_4$
30	30	30	5	5		
29.25	29.25	29.25	5.625	5.625	1	
22	6	39	2	2		29

Corrosion Database Development- Experiment Conditions

- ✓ Experiment conditions (gas composition and coal ash composition) were decided based on the analysis result and reported data in literature.
- ✓ 347H, component of the superheater, was obtained from Longview Power Plant

Representative chemical composition of the flue gas in literature

N_2	CO_2	SO_2	O_2	H_2O	HCl
81.25	15	0.25	3.5		
80	15	1	4		
Bal.	13.4	1300 vpm	4	8.6	400 vpm
80	10	1.5	3.5	5	
82.9	14	0.1	3		

Element composition of the 347H obtained from Longview Power Plant

Element	C	Mn	P	S	Si	Cr	Ni	Mo	Nb	Fe
Weight ratio (%)	0.041	1.75	0.02	0.003	0.32	17.52	9.22	0.26	0.71	Bal

Corrosion Database Development-Effect of Temperature

- ✓ OCP increases by time at 650 ^{o}C and 700 ^{o}C due to the growth of protective oxides (direct oxidation).
- ✓ It shows an opposite trend at 750 ^{o}C, decreasing from 603 mV to 520 mV due to the dissolution of protective scale.

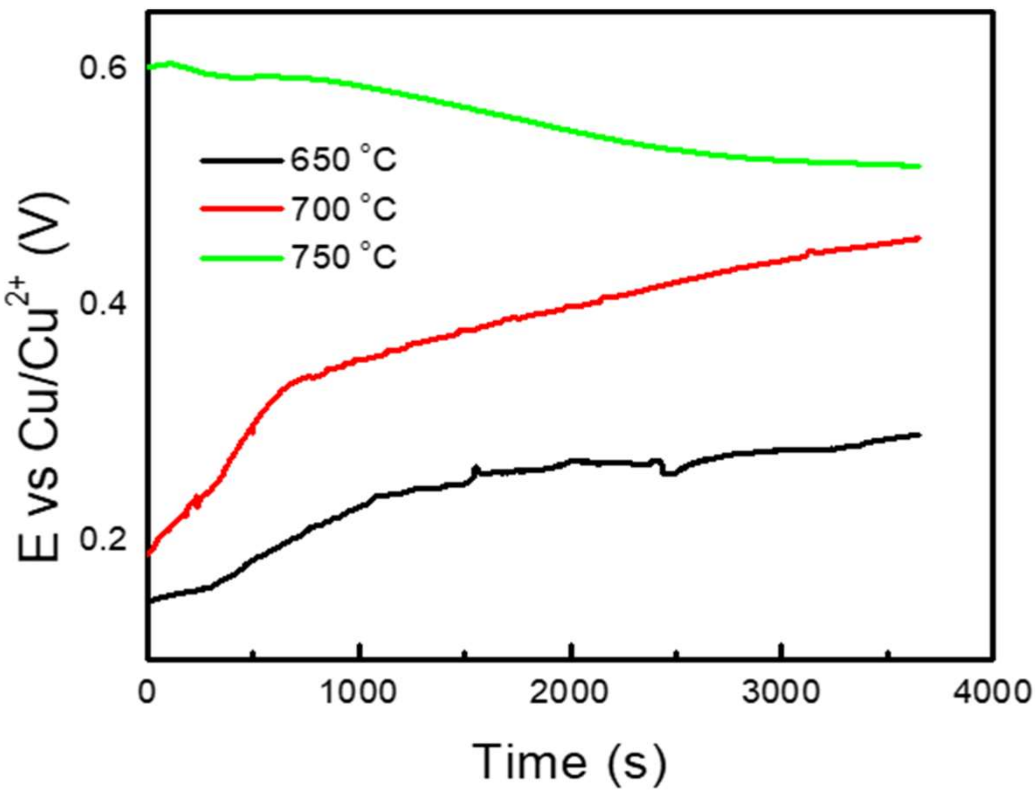

(a) OCP of 347H in the first 1h and (b) potentiodynamic polarization curve (PDP) at various temperature

Corrosion Database Development -Effect of Temperature

- ✓ Potential noise reveals two stages of the corrosion process: oxidation (increase of potential by time) and sulfidation (fluctuation of potential around 1.07 V).
- ✓ The sudden drop of potential at 700 ^oC is not recoverable while it recoveries after several hours at 750 ^oC.

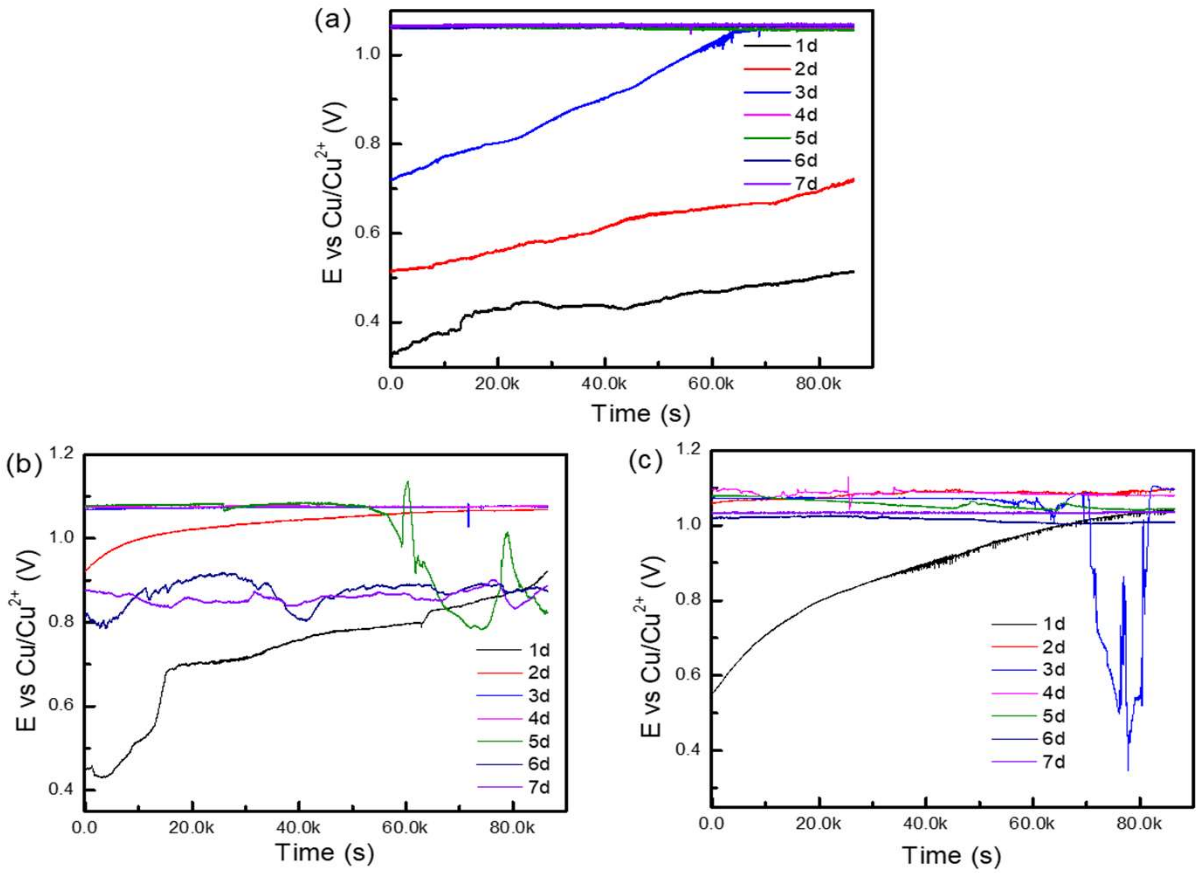

Time sequences of (a) potential and (b) current noise at 550 ^oC in a 7d exposure period

Corrosion Database Development -Effect of Temperature

- ✓ The current becomes stable when the potential approaches 1.07 V.
- ✓ The existence of numbers of spikes in current noise in the first few hours at 750 ^{o}C, suggesting the occurrence of pitting corrosion.

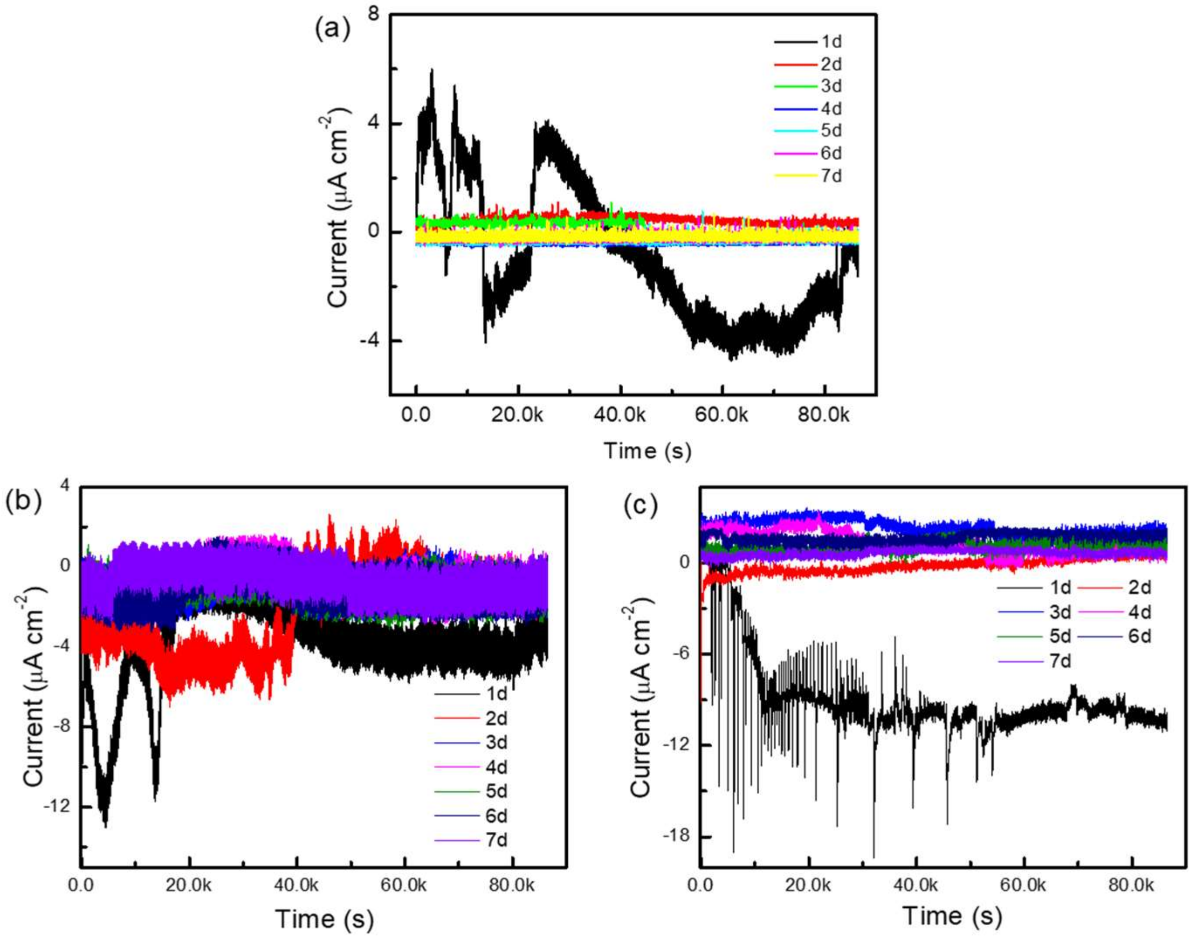

Time sequence of the electrochemical current noise at (a) 650^{o}C, (b) 700^{o}C and (c) 750^{o}C.

Corrosion Database Development -Effect of Temperature

- ✓ The minimum values of R_n and R_{sn} at 700 ^oC suggest that the corrosion rate is fastest at this experimental temperature
- ✓ Localized corrosion occurs in these working conditions.

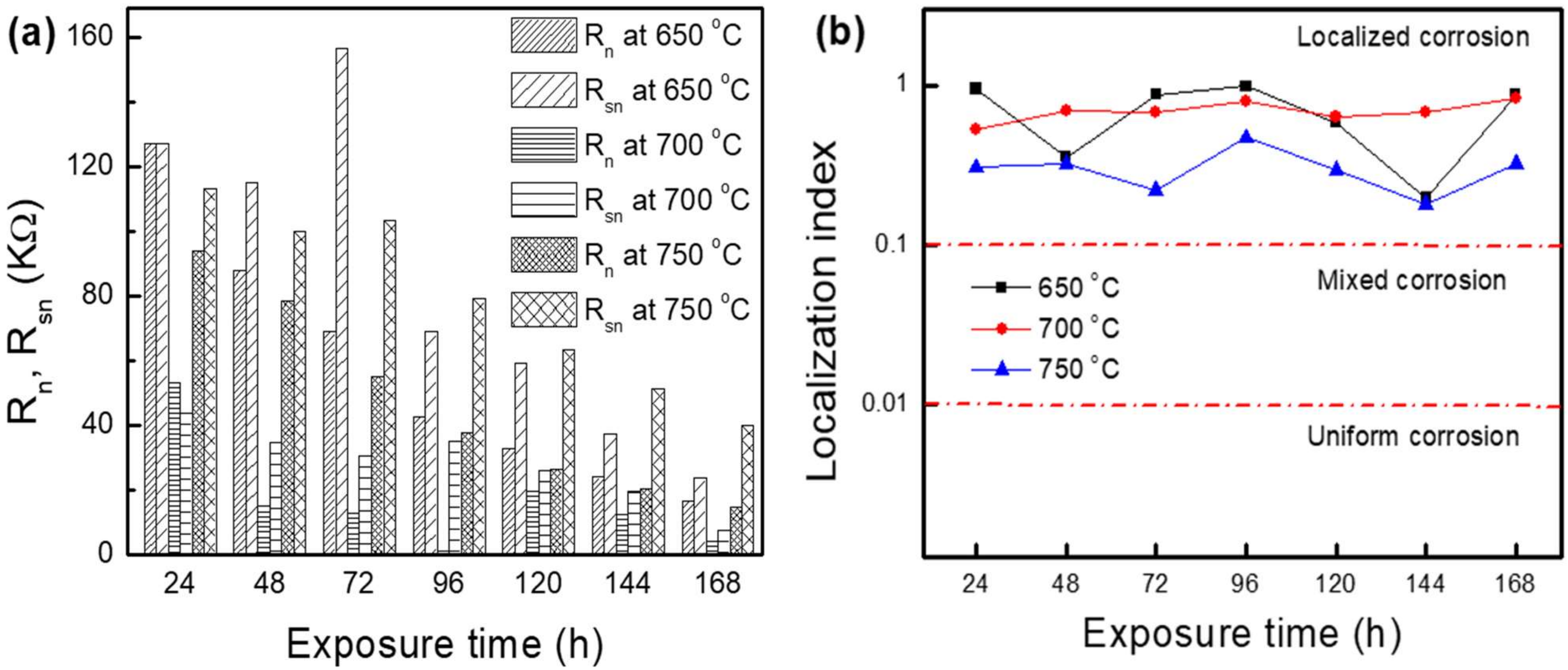

Comparison of (a) R_n and R_{sn} and (b) localization index at different temperatures

Corrosion Database Development -Effect of Temperature

✓ The current density in frequency domain at 700 ^{o}C is the highest, suggesting the fastest corrosion rate at 700 ^{o}C

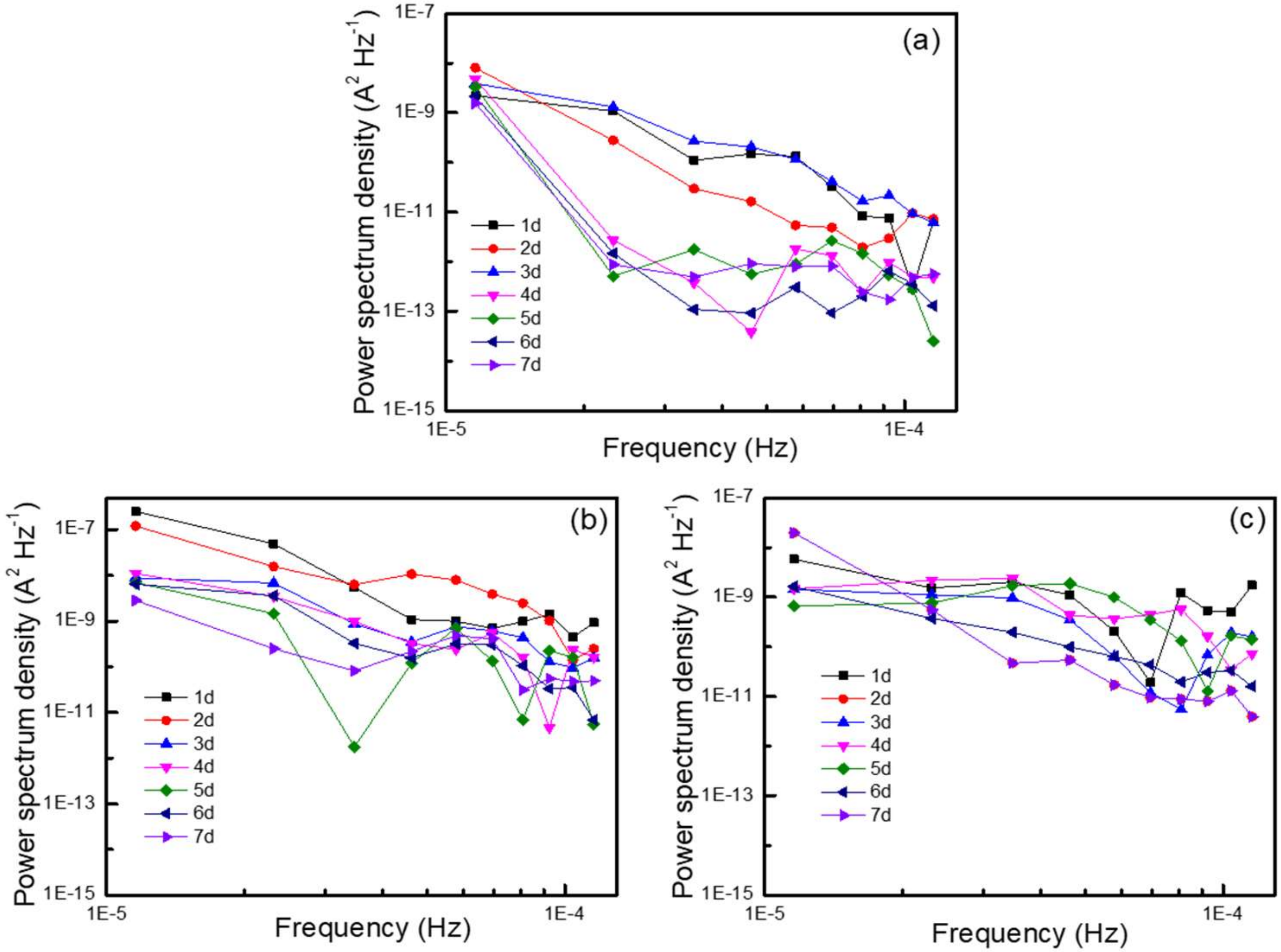

Frequency domain of the electrochemical current noise at (a) 650^{o}C, (b) 700^{o}C and (c) 750^{o}C.

Corrosion Database Development -Effect of Temperature

- ✓ Corrosion potential is lowest, and corrosion current density is highest at 700 °C, suggesting the poorest protection capability of the corrosion products at 700 °C
- ✓ It is impossible to quantitatively calculate the corrosion rate from the Tafel extrapolation method due to the limited Tafel region of the PDP curve.

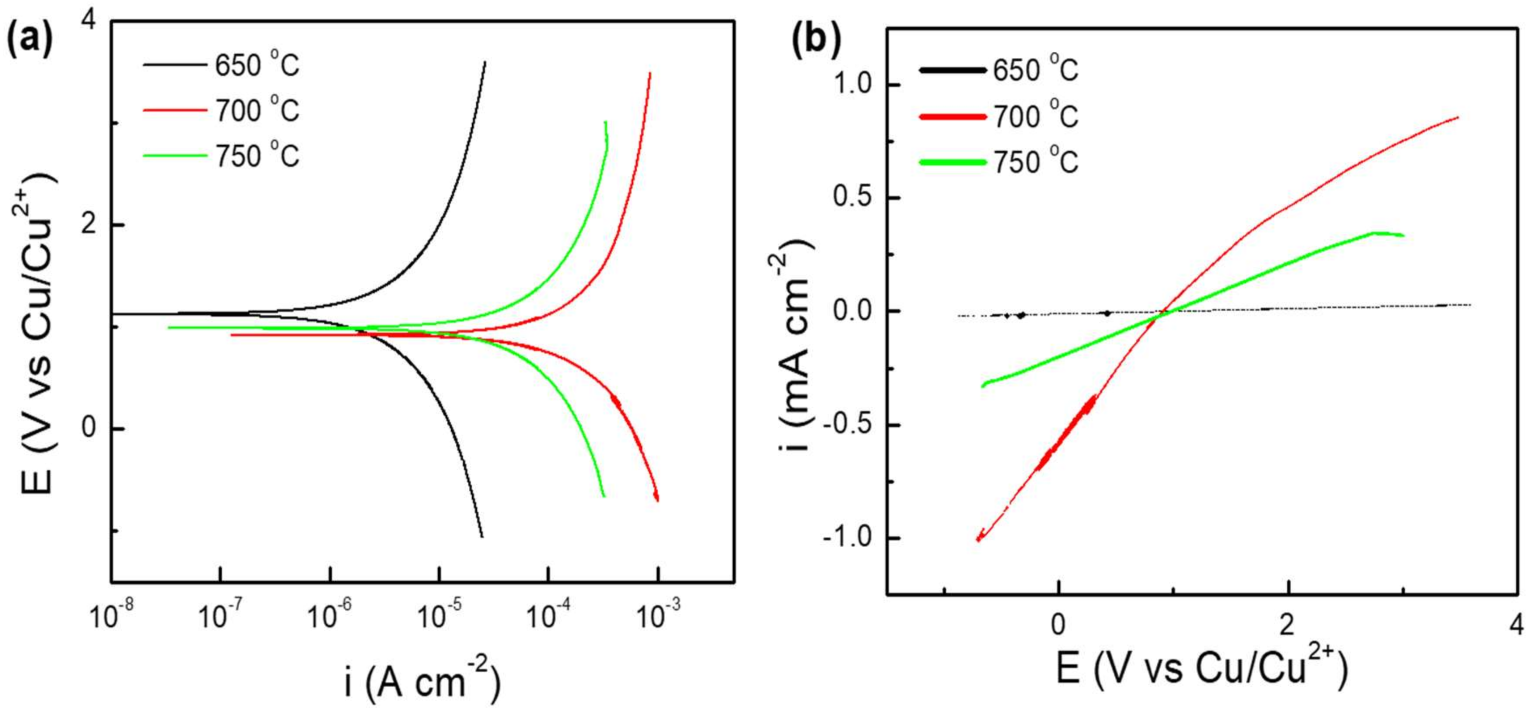

Potentiodynamic polarization curve and (b) corresponding i vs E plots at different temperatures.

Corrosion Database Development -Effect of Temperature

- ✓ The corrosion rate is fastest at 700 ^{o}C.
- ✓ This method can't provide accurate quantitative analysis in this system

$CR = (M \times i_{max})/Fn$

$D = CR \times 86400$

650 ^{o}C: 3.34 mg cm^{-2}

700 ^{o}C: 20.4 mg cm^{-2}

750 ^{o}C: 14.7 mg cm^{-2}

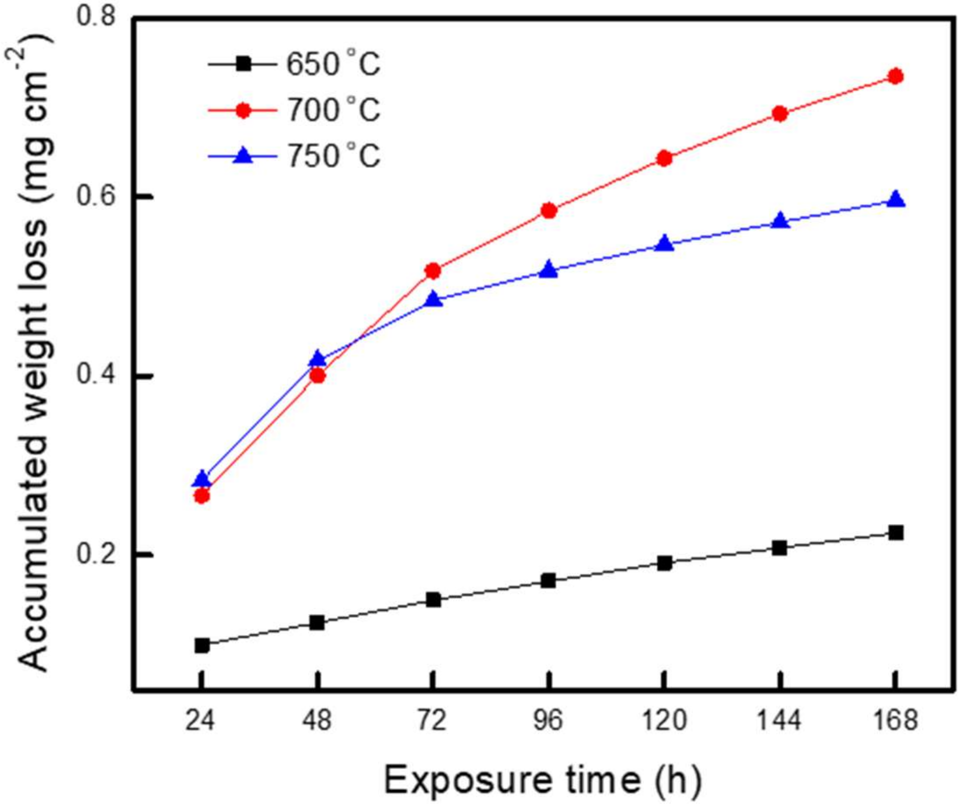

Accumulated corrosion rate calculated by EN data analysis at different temperatures.

Corrosion Database Development -Effect of Temperature

- ✓ The corrosion product consists of two layers, an outer layer mainly of chromium oxide and chromium sulfide, and an inner layer composed of iron oxide and iron sulfide regardless of the experimental temperature.
- ✓ The outer layer at 650 °C is much denser than that at 700 °C and 750 °C.

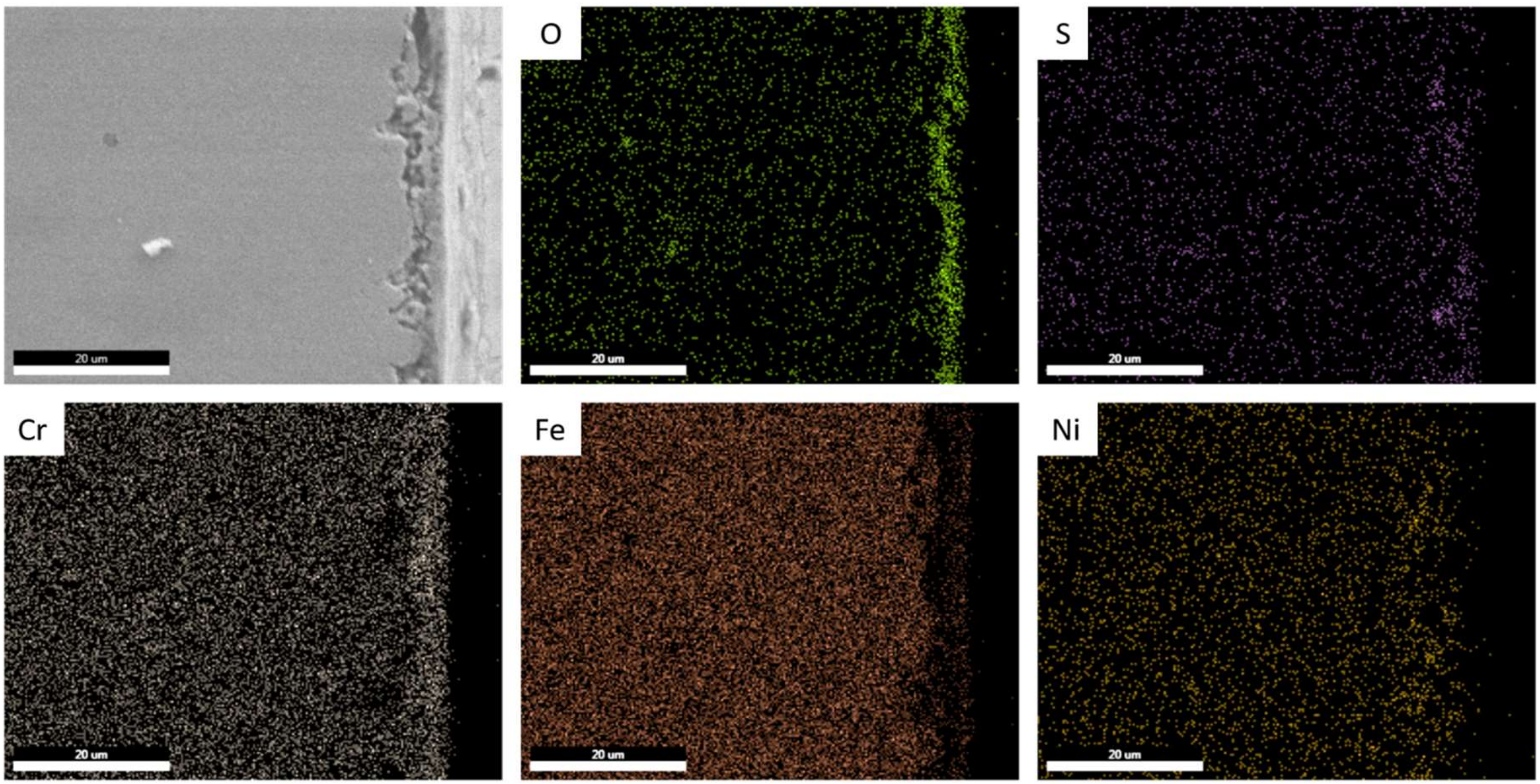

Cross section morphology and element distribution of TP347H after hot corrosion at 650 °C.

Techno-Economic Analysis - Motivation

- According to State of Reliability (SOR) report by North American Electric Reliability Council (NERC), coal-fired power plants' (CFPP) generation has the highest forced outage rate of all conventional fuels.
- Boiler tube leaks are one of the leading causes for forced outages.
- Waterwall tubes are one of the dominant locations for boiler tube leaks leading to about 6-7% loss in production time due to forced outages over past several years.

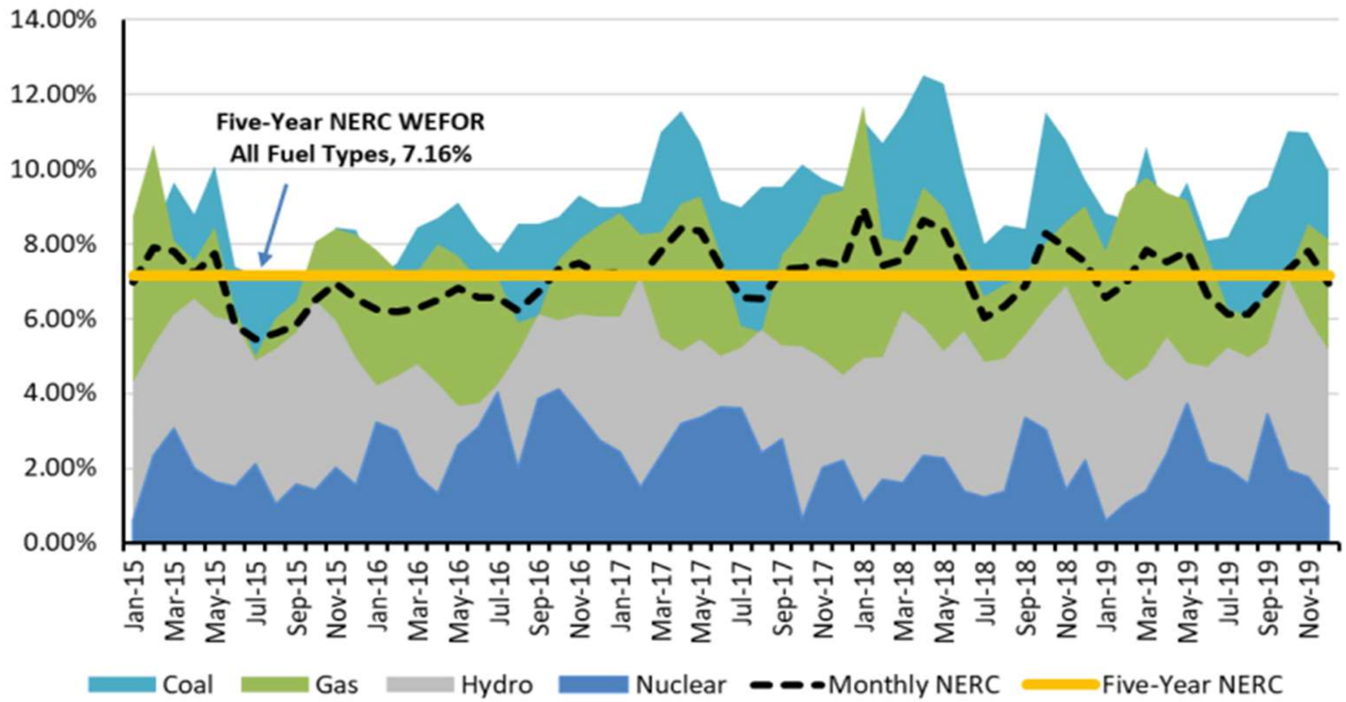

*Overlaid Monthly Capacity Weighted EFOR by Fuel Type, 2015-2019 **

* North American Electric Reliability Council (NERC), "State of Reliability," 2020.

TEA - Approach

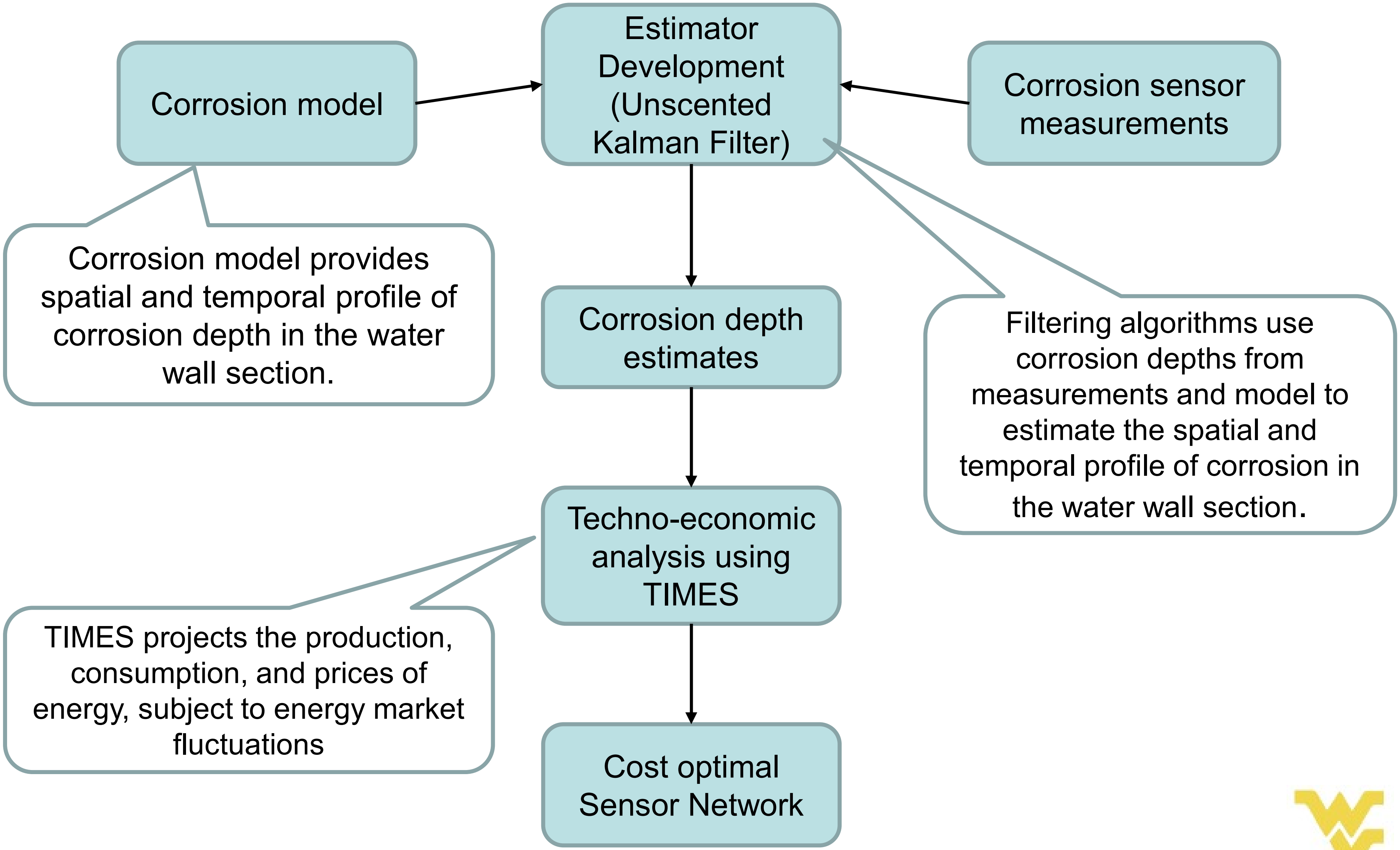

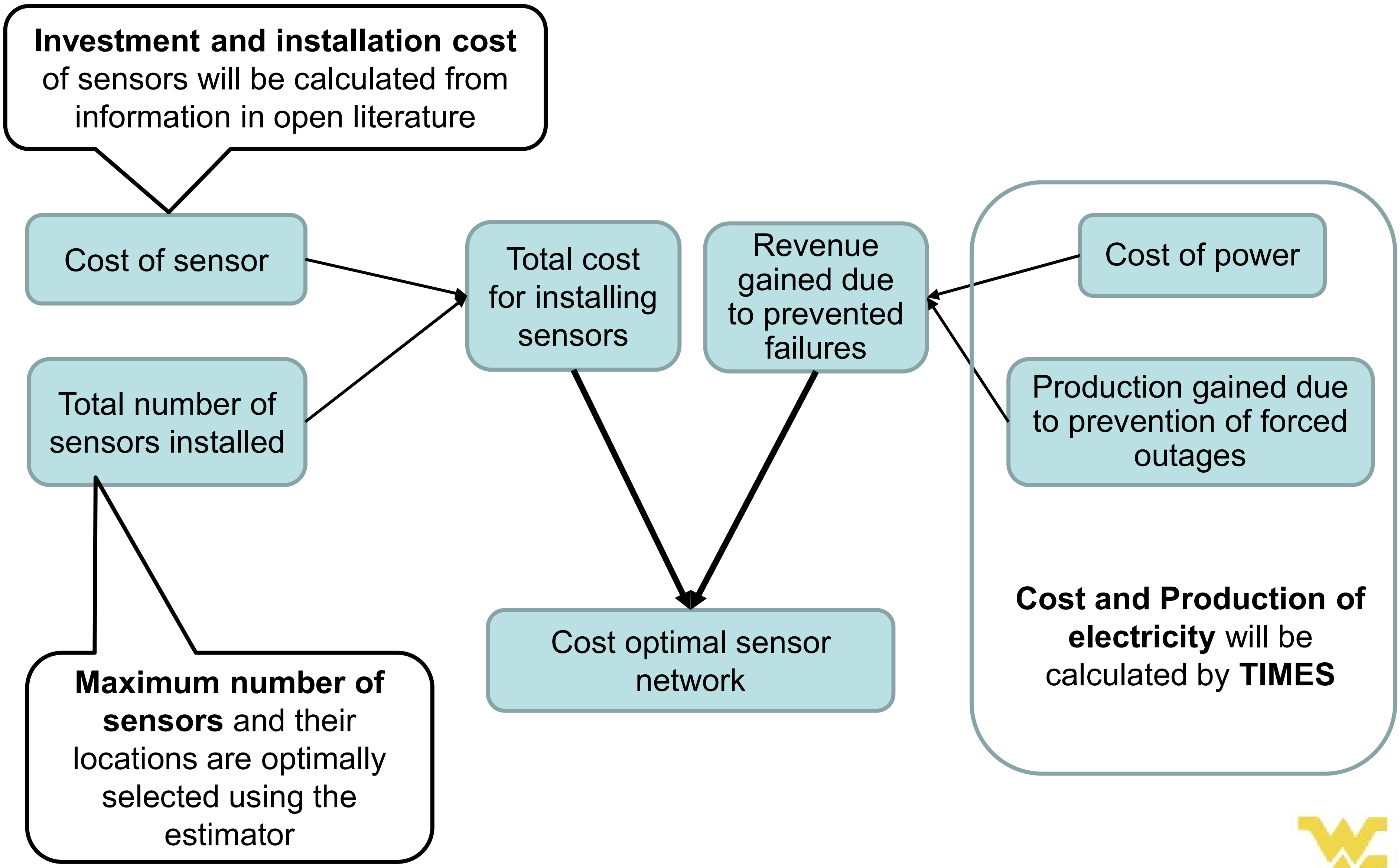

Investment and installation cost of sensors will be calculated from information in open literature
Cost of sensor
Total number of sensors installed
Maximum number of sensors and their locations are optimally selected using the estimator
Total cost for installing sensors
Revenue gained due to prevented failures
Cost optimal sensor network
Cost of power
Production gained due to prevention of forced outages
Cost and Production of electricity will be calculated by **TIMES**

TIMES Model

- **TIMES** model generator explores possible energy futures that meets the energy service demands, based on scenarios, inputs and constraints.
- The model representing U.S. energy system **‘EPAUS9rT’** was used.
- Base scenarios in EPAUS9rT were changed to mimic Annual Energy Outlook’s (AEO) considerations.
- Electricity produced by CFPP in the U.S. is computed by the EPAUS9rT model with and without modifications.

Aim is to find all combinations of scenarios under which potential revenue gained is more than the investment in sensor network.

Key technologies affecting CFPP’s generation are:

- Solar
- Wind
- Natural gas

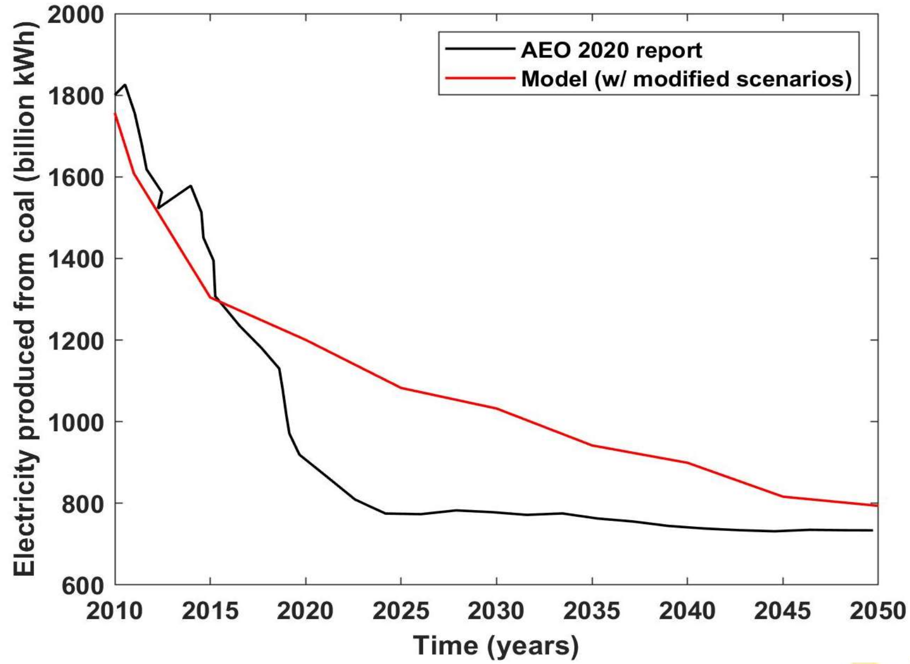

Comparison of amount of electricity generated from coal (billion kWh) from that of the AEO 2020 report, and EPAUS9rT model for reference case

TIMES Model - Results

- Electricity generated by CFPP under various cases with varying scenarios is calculated.
- In case 1 and case 2, only coal power plants have been incentivized. In case 3, additional scenarios that may constrain the growth of solar technology is included, as an extremity scenario.
- From case 1 to case 3, the CFPP's generation has increased progressively. The study shows that the other power generation technologies can also significantly affect the availability of coal plants.

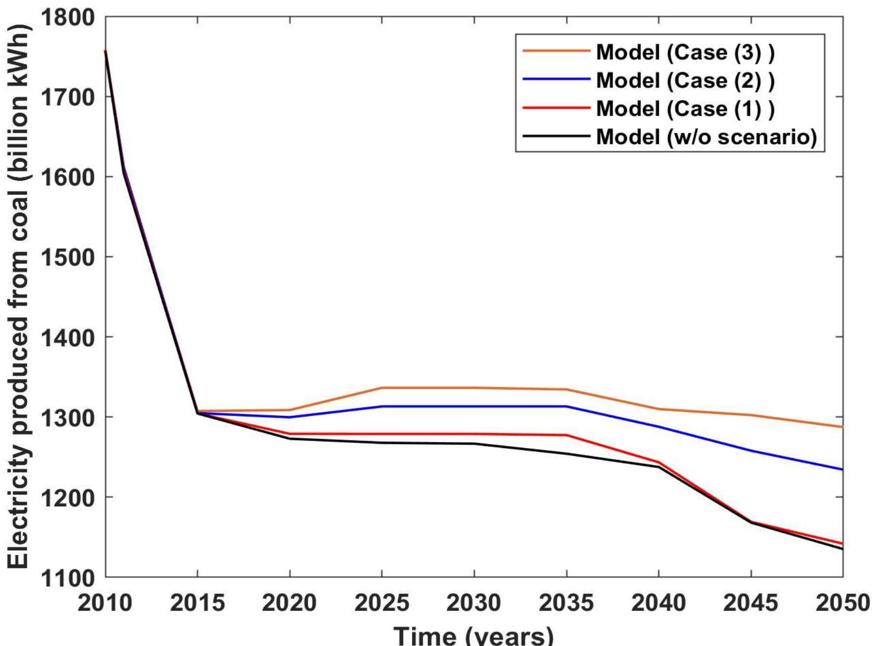

Comparison of amount of electricity generated from coal (billion kWh) from EPAUS9rT model under various cases

Case Number	Technologies				
	Coal		Solar		
	Availability	Fixed O&M	Fixed O&M	Investment cost	Availability
Case 1	↑ 50%	-	-	-	-
Case 2	↑ 50%	↓ 30%	-	-	-
Case 3	↑ 50%	↓ 30%	↑ 40%	↑ 30%	↓ 30%

List of the cases and their corresponding scenarios implemented in EPAUS9rT model execution

- Each case has scenarios that deal with the same wind, solar, and natural gas technologies. But the degree of deviation from reference case varies.
- In Case 1, very high growth in renewables is considered while in Case 3 there is no significant growth. These are two extremities. Case 3 represents medium level growth in renewables.
- Degree of growth of renewables has strong impact on the CFPP's generation.
- Hence, a preliminary set of uncertainties that impact CFPP's generation have been identified and evaluated.

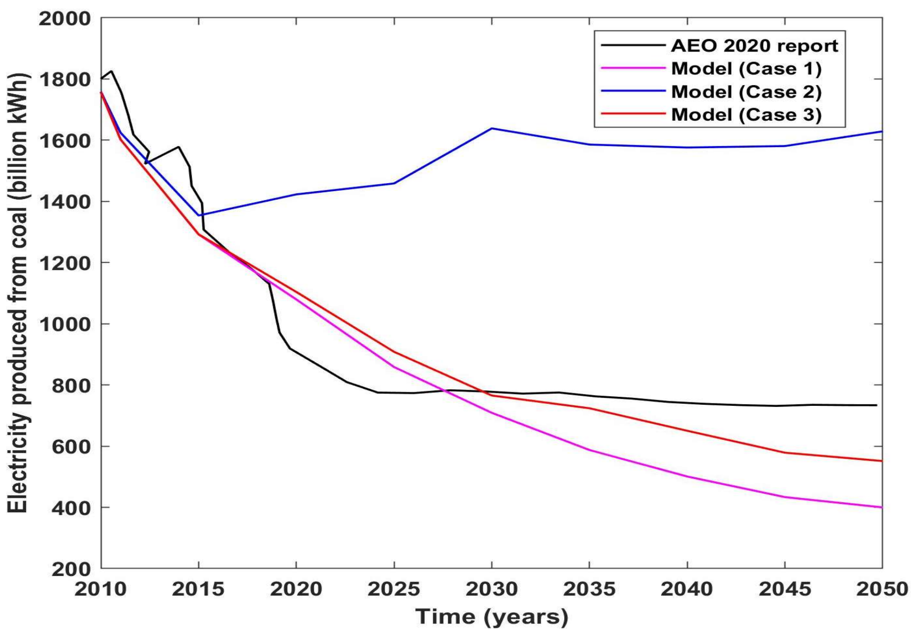

Comparison of amount of electricity generated from coal (billion kWh) from that of the AEO 2020 report, and EPAUS9rT model under the three cases

Case Number	Technologies			
	Solar		Wind	
	Fixed O&M	Investment cost	Fixed O&M	Investment cost
Case 1	↓ 75%	↓ 75%	↓ 80%	↓ 70%
Case 2	↑ 120%	↑ 100%	↑ 110%	↑ 110%
Case 3	↓ 65%	↓ 70%	↓ 77%	↓ 67%

List of the cases and their corresponding scenarios implemented in EPAUS9rT model execution

Cost-Optimal Sensor Network Synthesis

- Wireless networks can suffer from packet drop off and/or loss of data, leading to missing measurements at various instances of time.
- Sensitivity study was conducted to find the impact of missing measurements on corrosion depth estimate's accuracy.
- Sensitivity study indicated that filter estimates were accurate up to about 80% data loss for a given sensor network.

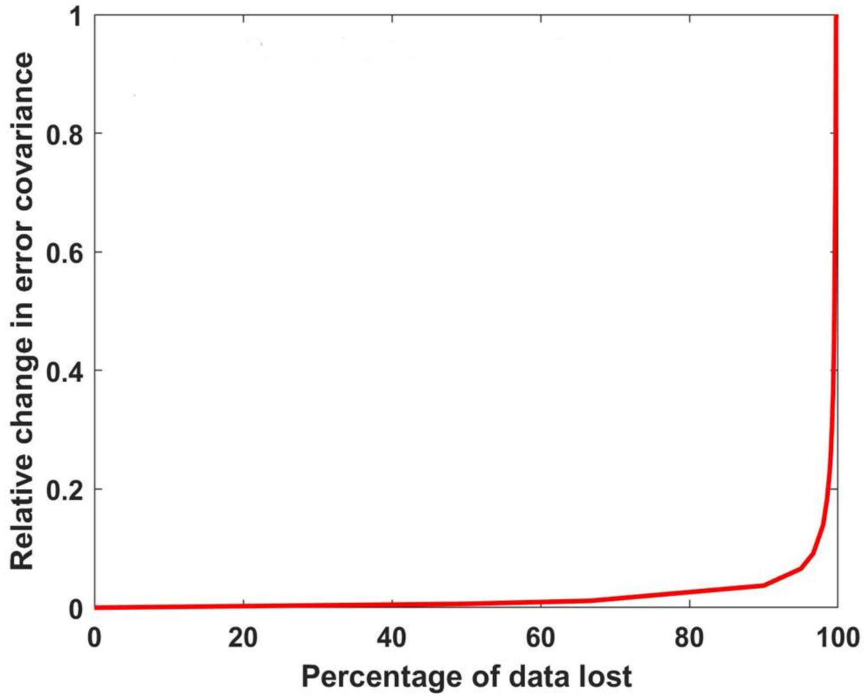

The sensitivity of relative change in error covariance of corrosion depth with missing measurement to the percentage loss in data transmitted by sensor

- A cost-optimal sensor network synthesis algorithm is at the final stage of development.

- Sensor measurements using an Unscented Kalman filter (UKF) improve the estimates of tube thickness even in the presence of large model mismatch thus providing a good estimate of failure time.

- The cost-optimal sensor network considers the tradeoff between the cost of the sensor network versus the improved profitability due to higher availability and lower unplanned outage while considering the uncertainties in the availabilities in the renewables.

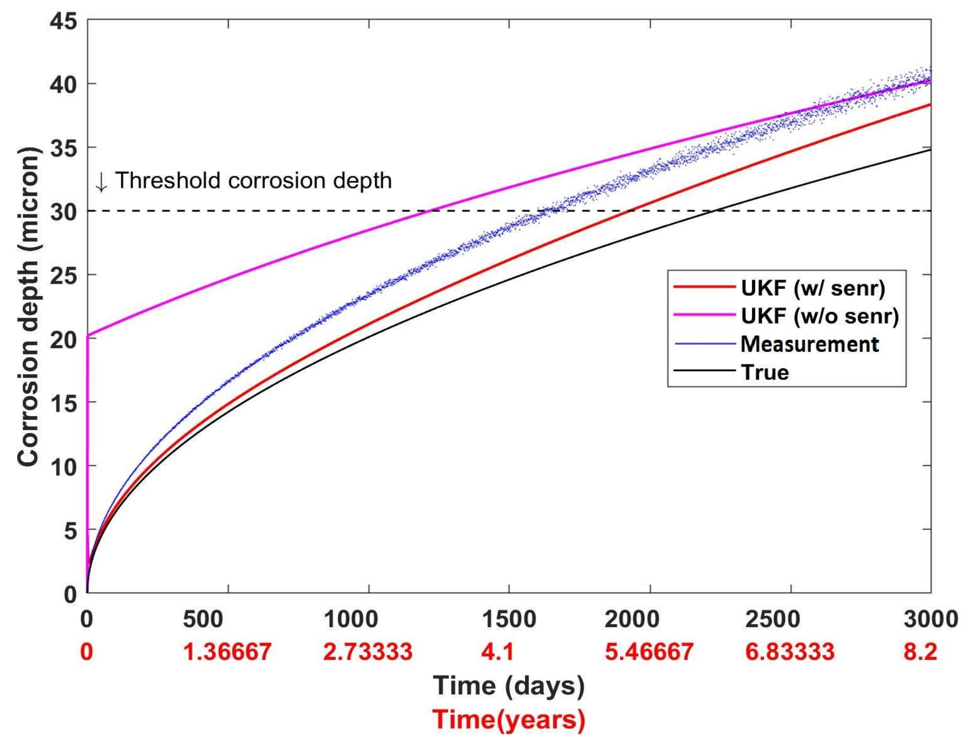

Comparison of the UKF estimate of corrosion depth (micron) calculated with and without measurements, with that of the true and measured corrosion depths with time, at certain location of waterwall

SUMMARY & FUTURE WORK

Progress-to-date

- Last sensors has been running @ Longview for seven month with good performance
- Remote data collection has been enabled and data obtained seems to be stable & reasonable
- Real time corrosion monitoring has been realized
- A predictive model has been developed to calculate the corrosion rate by EN data
- Lab-scale RE with good stability and reproducibility has been developed.
- Corrosion database development and techno-economical analysis (TEA) are ongoing in schedule.

Future work

- Incorporate the new RE in the sensor @ Longview.
- Continue corrosion database development.
- Continue techno-economical analysis (TEA)

AKNOWLEDGEMENT

DoE-NETL:

- DE-FE 05717: Bob Romanosky, Susan Maley, Chuck Miller, etc.
- DE-FE 31548: John Rockey, Briggs White, Sydni Credle, Jessica Mullen, etc.

Collaborators and Partners:

- WRI - Don Collins, Vijay Sethi
- Special Metals - Jack deBarbadillo, Brian Baker, Gaylord Smith
- ILZRO - Frank Goodwin
- NETL-Albany - Paul Jablonski, Jeff Hawk, Gordon Holcomb, Dave Alman etc.
- Longview Power – Jared Custer, Chad Hufnage, Jeffrey Westfall
- Aspinity - Brandon Rumberg, Don Boucher

AKNOWLEDGEMENT

This material is based upon work supported by the Department of Energy Award Number DE-FE0031548."